

A computational study on radiation shielding performances of self-passivating tungsten alloys

Zeynep Aygun^{1*}, Murat Aygun²

¹Bitlis Eren University, Vocational School of Technical Sciences, Bitlis, Turkey.

²Bitlis Eren University, Faculty of Science and Arts, Department of Physics, Bitlis, Turkey.

*Corresponding author: zeynep.yarbasi@gmail.com

Received 09 March 2023; Accepted 11 August 2023; Published Online 15 September 2023 ORIGINAL RESEARCH

Abstract:

Tungsten with its superior features such as high melting point and relatively high thermal conductivity is significant for many high temperature applications. The materials, including tungsten, which have important mechanical properties should also be investigated by their radiation attenuating abilities. The goal of the study is to contribute to the carried out studies from a different perspective by calculating radiation-matter interaction parameters of self-passivating tungsten alloys. Radiation shielding capabilities of the alloys were determined in the range of 1 keV - 100 GeV by Phy-X/PSD code. XCOM, a well-known code, was also used for seeing the validity of obtained mass attenuation coefficients of the alloys. It was observed that half value layer and mean free path values of the studied alloys are lower, and mass attenuation coefficients are higher than those of previously reported alloys. The alloys with higher amounts of tungsten and yttrium have higher shielding ability, while the alloys with lighter elements titanium and silica have less. Additionally, depending on the obtained fast neutron removal cross section values, the studied self-passivating tungsten alloys can be also evaluated for neutron shielding. It can be concluded that the self-passivating alloys have good radiation protection potentials besides the significant mechanical properties.

Keywords: Radiation attenuation parameters; SPWAs; Phy-X/PSD

1. Introduction

There is a great interest for tungsten (*W*) which has the highest melting point and tensile strength and relatively high thermal conductivity of all metals [1]. These features make the element important for the high temperature applications like concentrated solar power, power generation, and materials of future fusion reactors. However, the property of low oxidation resistance limits the use of *W* in a vacuum or oxidizing environments to temperatures below 500°C [2]. Recently, extensive studies are carried out for the design of the future fusion power plant around the world. The components and materials chosen for the design of the fusion power plant require high safety and operational standards [3]. In the existence of a possible loss-of-coolant accident in the reactor, a temperature increase can be occurred around 1000 – 1200°C [2]. This case causes a quick oxidation of the pure *W* surface and can form highly radioactive WO_3 . In order to get rid of this problem, many researchers prefer to develop self-passivating *W* alloys by

using elements such as titanium (Ti), silica (Si), niobium (Nb), chromium (Cr), yttrium (Y) and zirconium (Zr) which have stable thermodynamic characteristics and low neutron irradiation activation [2–7]. A protective oxide scale can be obtained and the further oxidation of the *W*-based alloys can be delayed by adding these elements. Calvo et al. reported that $W_{10}Cr_{0.3}Y$ SPWA has the highest oxidation rate, while $W_{10}Cr_{1}Y$ has the lowest oxidation rate [2]. $W_{10}Cr_{0.5}Y$ and $W_{8}Cr_{0.5}Y$ have similar rates. Sal et al. stated that the addition of Zr ($W_{10}Cr_{0.5}Y_{0.5}Zr$) is not sufficient to vary the oxidation features of the $W_{10}Cr_{0.5}Y$ alloy [8]. The result of SPWA with Ti content has more oxidation resistance comparing with WCr alloy was mentioned by Garcia-Rosales et al. [5]. It was stated that self-passivating *W* smart alloys are composed of Cr as a passivating element and a small amount of Y as an active element which has several favorable effects on both durability and stability of alloys [9].

As the first wall armor of future fusion reactors is planned to be designed with SPWAs, it can be said that the results

Table 1. The chemical contents of SPWAs samples.

Alloy	W	Cr	Y	Ti	Zr	Si	Density (g/cm ³)
S1	87.8	11.6	0.6	-	-	-	17.823
S2	88	10	-	2	-	-	17.817
S3	89.5	10	0.5	-	-	-	18.027
S4	80	10	-	-	-	10	15.700
S5	85.5	12	-	2.5	-	-	17.509
S6	89.7	10	0.3	-	-	-	18.091
S7	89.5	10	-	-	0.5	-	18.086
S8	89	10	1	-	-	-	17.866
S9	91.5	8	0.5	-	-	-	18.240
S10	89	10	0.5	-	0.5	-	17.928

of the research are directly beneficial in nuclear technology. The use of nuclear technology, which is of interest to the whole world, has also made the subject of radiation shielding interesting. The relation between the technology and radiation shielding leads to the production of new radiation shielding materials. Recently, various materials such as glasses, alloys, composites, rocks, concretes etc. have been developed and investigated for radiation attenuating potentials [10–21]. It is essential to determine the radiation protection parameters in order to identify the efficiency of a radiation shielding material. The parameters are linear attenuation coefficient (LAC), mass attenuation coefficient (MAC), effective atomic number (Z_{eff}), mean free path (MFP), half value layer (HVL), total atomic cross section (ACS), total electronic cross section (ECS), fast neutron removal cross section (FNRCs) and buildup factors (EBF and EABF). XCOM [22], XMuDat [23], WinX-Com [24, 25], Geant4 [26], Phy-X/PSD [27], EpiXS [28], and Py-MLBUF [29] are the programs generally used for determination of radiation attenuation parameters.

The objective of the study is to determine the radiation attenuation parameters of recently developed self-passivating W alloys (SPWA) which were widely studied by their microstructure, oxidation behavior, and failure mechanisms previously [2, 8, 9, 30, 31]. Phy-X/PSD code was used for calculation of the parameters. The radiation-matter

interaction parameters of materials can be determined between the energies from 1 keV to 100 GeV by inserting the chemical composition and density of the material. Numerous researches about radiation shielding characteristics of materials have been carried out by performing the program [13, 15, 17, 32, 33]. Obtaining the radiation protection parameters of the alloys will be important in terms of providing information about the alloys, called as smart alloys, to the literature. This work adds an important contribution to the research areas related with nuclear and fusion technology by investigating new type of alloys whose negative effects can be eliminated that may be encountered at high temperatures. The analysis will have significant implications for the use of alloys as good radiation shields at higher temperatures in a variety of applications. Besides the theoretical evaluation, giving experimental results may be supportive and can be done in future studies.

2. Materials and methods

In the study, the chemical contents of SPWAs were acquired from the literature [2, 8, 9, 30, 31] and are given in Table 1. The rule of mixture is used for the determination of density (ρ_{mix}) of the alloys [34]:

$$\rho_{mix} = \frac{\sum_{i=1}^n c_i A_i}{\sum_{i=1}^n \frac{c_i A_i}{\rho_i}} \quad (1)$$

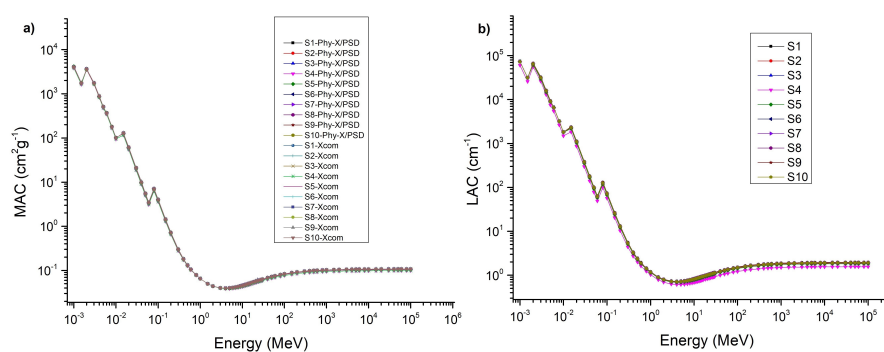


Figure 1. The variations of MAC (a) and LAC (b) values of the SPWAs versus photon energies.

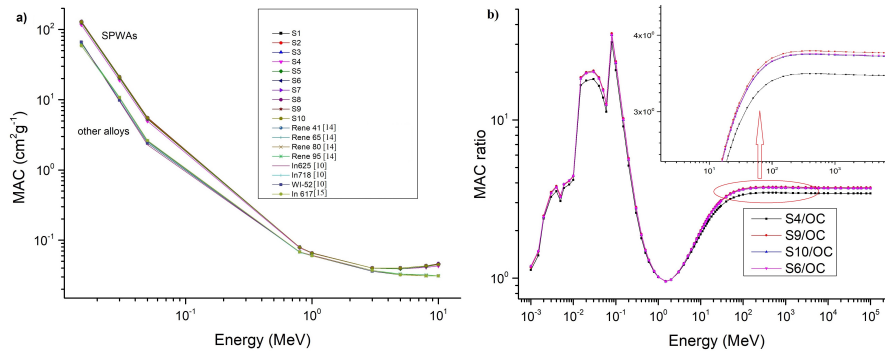


Figure 2. The variations of MAC values of the SPWAs and previously studied alloys (a) and the ratio of MAC values (b) versus photon energies.

A_i , c_i and ρ_i , and are atomic fraction, atomic weight of element i_{th} and density, respectively.

The MAC can be calculated based on the Beer–Lambert as:

$$I = I_0 e^{-\mu t} \tag{2}$$

$$\mu_m = \frac{\mu}{\rho} = \frac{\ln \frac{I}{I_0}}{\rho t} = \frac{\ln \frac{I}{I_0}}{t_m} \tag{3}$$

where t (cm), t_m (g/cm²), μ (cm⁻¹) and μ_m (cm²/g) are the thickness and sample mass thickness (the mass per unit area), LAC and MAC, respectively.

For any compound, MAC can be also acquired by the following equation [27];

$$\frac{\mu}{\rho} = \sum_i w_i \left(\frac{\mu}{\rho}\right)_i \tag{4}$$

where $(\mu/\rho)_i$ and w_i are the MAC of the i_{th} constituent element and the weight fraction, respectively.

MFP and HVL can be determined by the formulas,

$$\text{MFP} = \frac{1}{\mu} \tag{5}$$

$$\text{HVL} = \frac{\ln(2)}{\mu} \tag{6}$$

ACS (σ_a) can be calculated by the equation given as;

$$\text{ACS} = \sigma_a = \frac{N}{N_A} (\mu/\rho) \tag{7}$$

ECS (σ_e) is formulated by the following equation;

$$\text{ECS} = \sigma_e = \frac{\sigma_a}{Z_{eff}} \tag{8}$$

Z_{eff} is found by the help of Eqs. (7) and (8) as;

$$Z_{eff} = \frac{\sigma_a}{\sigma_e} \tag{9}$$

EBF and EABF can be calculated by the given equations below [35, 36]. The geometric progression (G-P) fitting parameters can be calculated by using values [37] in Eq. 14. EBF and EABF can be obtained using Eq. (12) or (13) by obtaining $K(E, x)$ in Eq. (14), where a, b, c, d and X_k are the exposure GP fitting parameters and x is thickness in mean free path (mfp). The ratio (R) of Compton partial MAC to total MAC should be defined for the material at specific energy. The R_1 and R_2 values indicate the $(\mu m)_{\text{Compton}}/(\mu m)_{\text{Total}}$ ratios of these two adjacent elements which have Z_1 and Z_2 atomic numbers. F_1 and F_2 are the values of G-P fitting parameters identical with the Z_1 and Z_2 atomic numbers at a certain energy, respectively. E and X demonstrate primary photon energy and penetration depth, respectively.

Combination of $K(E, X)$ with X , performs the photon dose multiplication and determines the shape of the spectrum.

$$Z_{eq} = \frac{Z_1(\log R_2 - \log R) + Z_2(\log R - \log R_1)}{\log R_2 - \log R_1} \tag{10}$$

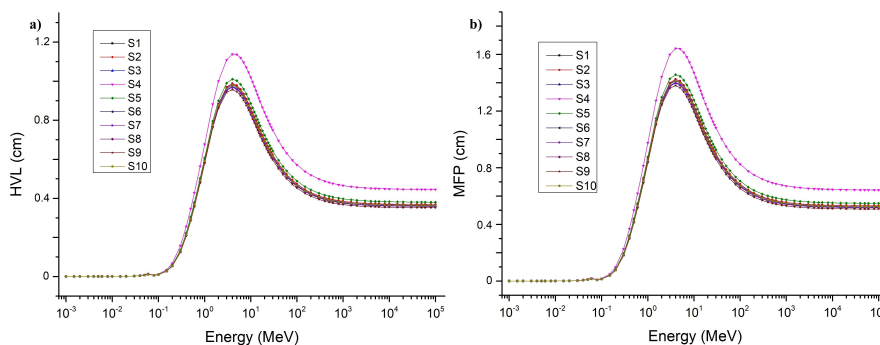


Figure 3. The variations of HVL (a) and MFP (b) values of the SPWAs versus photon energies.

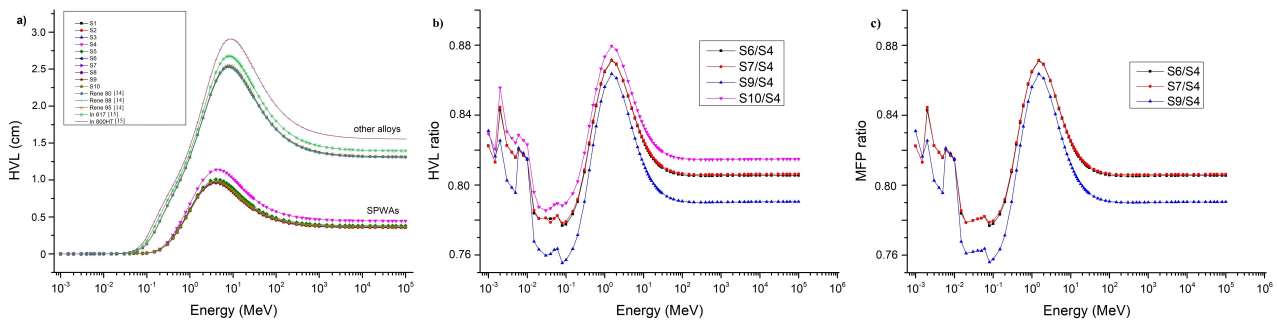


Figure 4. The variations of HVL values of the SPWAs and previously studied alloys (a) and the ratio of HVL (b) and MFP values (c) versus photon energies.

$$F = \frac{F_1(\log Z_2 - \log Z_{eq}) + F_2(\log Z_{eq} - \log Z_1)}{\log Z_2 - \log Z_1} \quad (11)$$

$$B(E, x) = 1 + \frac{(b-1)(K^x - 1)}{K - 1} \text{ for } K \neq 1 \quad (12)$$

$$B(E, x) = 1 + (b-1)x \text{ for } K = 1 \quad (13)$$

$$K(E, x) = cx^a + d \frac{\tanh(\frac{x}{X_k} - 2) - \tanh(-2)}{1 - \tanh(-2)} \text{ for } x \leq 40 \text{ mfp} \quad (14)$$

The FNRCs ($\sum R$) values of the compounds are determined as follows [38, 39]:

$$\sum R = \sum_i \rho_i \left(\frac{\sum R}{\rho} \right)_i \quad (15)$$

where ρ_i and $(\sum R/\rho)_i$ are the partial density of the compound and the mass RCS of the i^{th} constituent element, respectively.

3. Results and discussion

The radiation-matter interaction parameters of SPWAs were obtained by using Phy-X/PSD code. Changes of the MAC results versus photon energies (1 keV - 100 GeV) are shown in Fig. 1(a). Due to the fact that photoelectric effect (PE),

Compton scattering (CS) and pair production (PP) are dominant at low, mid energies and energies > 5 MeV, respectively, the variations of MAC are observed as given in Fig. 1(a). The MAC values were also obtained by XCOM [22], and the values calculated by the codes are compatible. Since, the achieved MAC values of SPWAs are very close to each other, in order to learn clearly which alloy has more shielding potential, the ratio of MAC values of the SPWAs with highest shielding properties (S6, S9 and S10) and that with lowest one (S4) to a reference material ordinary concrete (OC) [40] is obtained. It is obvious that the MAC values of S6, S9 and S10 are the highest among the alloys. Change of the LAC values as a function of photon energies (1 keV - 100 GeV) is given in Fig. 1(b). Since, LAC parameter is attached to both MAC and density of material, the lowest LAC values are determined for S4 alloy with lowest density at all energies. In order to make an expressive evaluation, MAC values of the SPWAs are compared with those of other alloys (Fig. 2(a)). It can be clearly seen that the obtained MAC values of SPWAs (upper group lines) are higher than those of previously reported alloys (subgroup lines). The ratio of MAC values of the SPWAs (S4, S6, S9 and S10) to the those of OC is shown in Fig. 2(b) in order to see the shielding efficiency of the alloys. However, the MAC values of S6, S9 and S10 are seemed very close, a specific energy region on the graph is shown in a separate window and it is observed that S9 alloy has the highest ratio among them. Therefore, it can be concluded that S9 has more shielding ability.

The capability of radiation to penetrate materials can

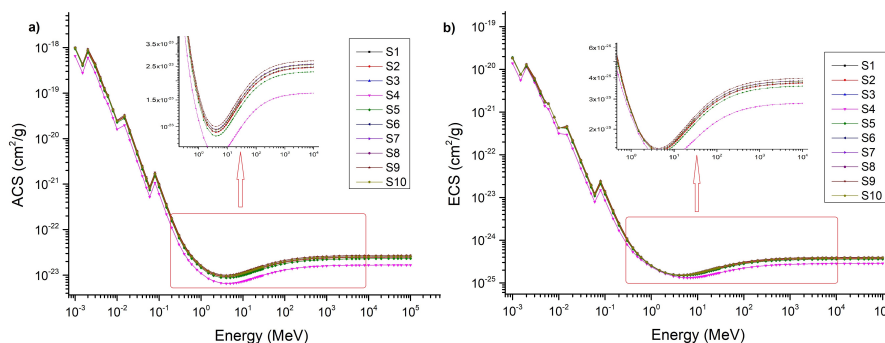


Figure 5. The changes of ACS (a) and ECS (b) versus photon energies.

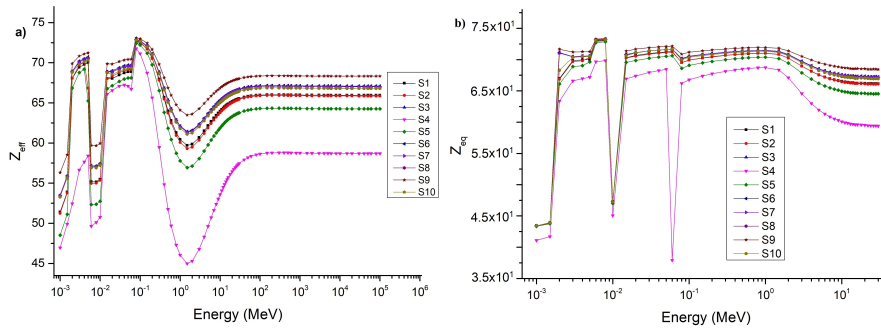


Figure 6. The variations of Z_{eff} (a) and Z_{eq} (b) versus photon energies.

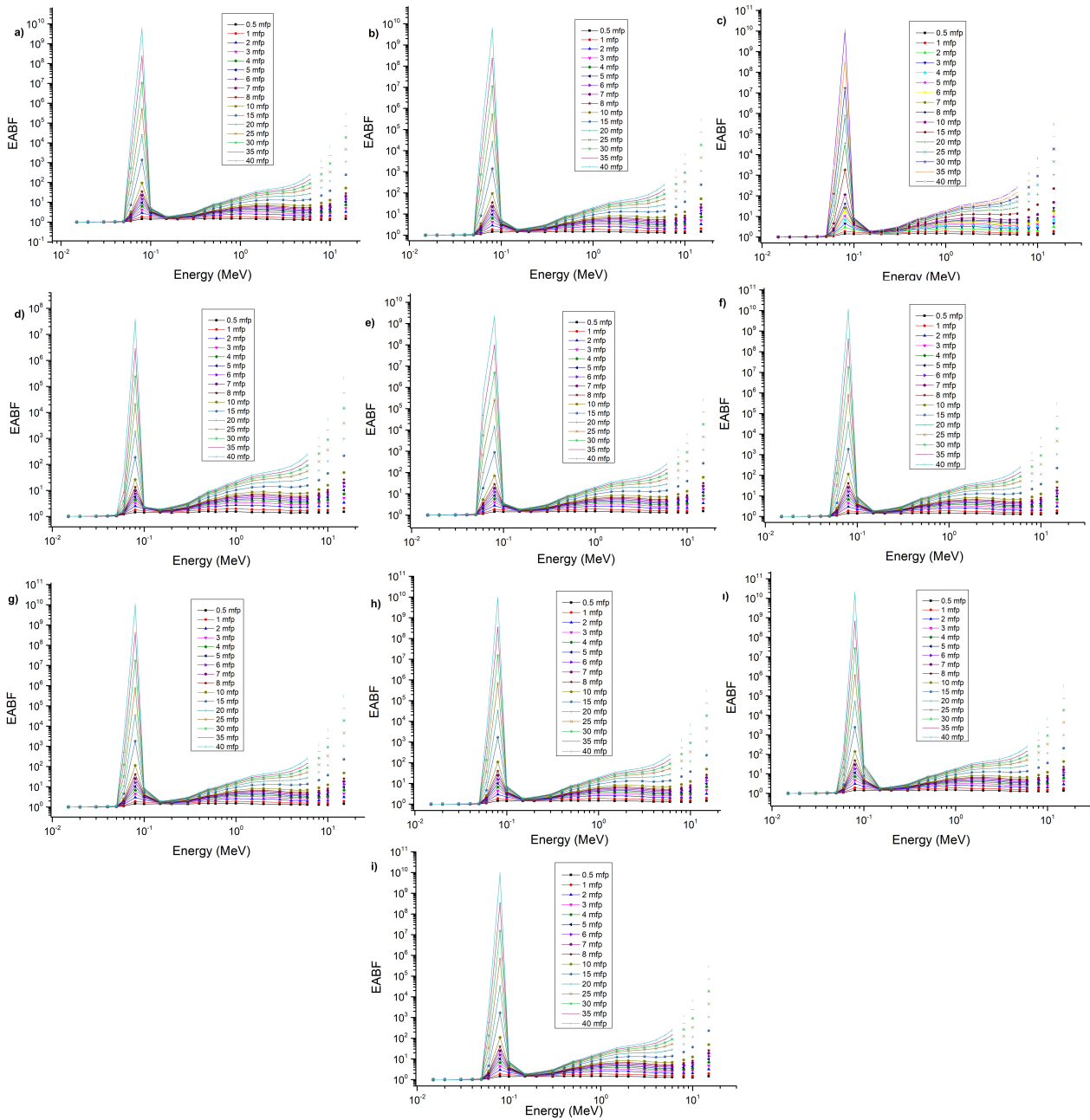


Figure 7. The changes of EABF for S1 (a) S2 (b) S3 (c) S4 (d) S5 (e) S6 (f) S7 (g) S8 (h) S9 (i) S10 (i) versus photon energies.

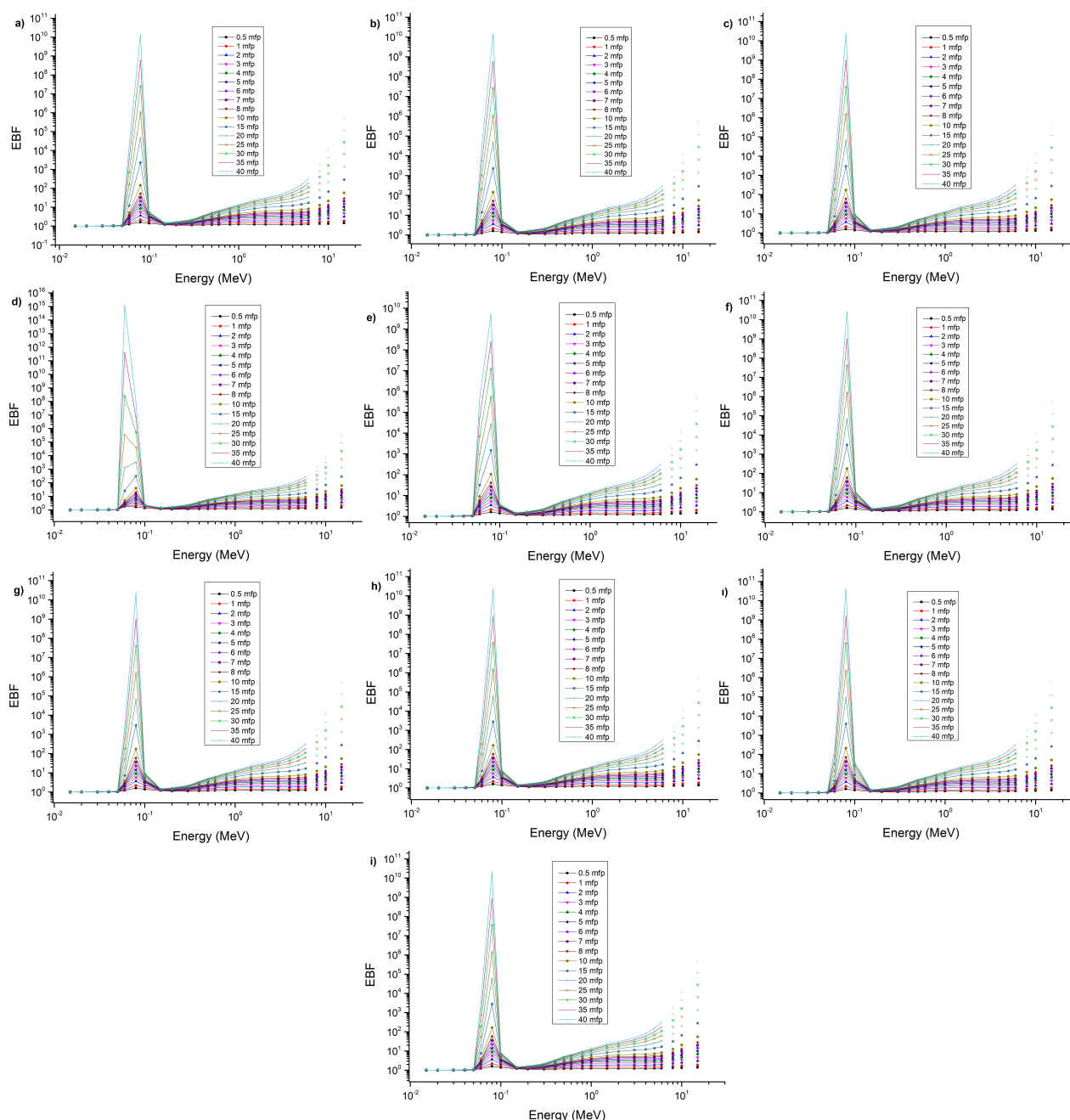


Figure 8. The changes of EBF for S1 (a) S2 (b) S3 (c) S4 (d) S5 (e) S6 (f) S7 (g) S8 (h) S9 (i) S10 (i) versus photon energies.

be given by HVL parameter. The MFP parameter represents the average distance traveled by the radiation between two successive collisions in the compound. Dependences of MFP and HVL parameters versus photon energies are shown in Fig. 3. It is desired to have lower HVL and MFP values of materials in the high energy regions for better shielding property. It is obtained that HVL and MFP results of the SPWAs are very close to each other except from S4. The highest values of HVL and MFP are determined for S4 depending on the density value of the alloy. The photon shielding effectiveness of the alloys are analyzed by comparing HVL values of SPWAs and other studied alloys (Fig. 4(a)). It is obviously noted that the obtained HVL results (subgroup lines) are lower than those of previously reported

alloys (upper group lines). Additionally, for the purpose of evaluating the shielding performances of the alloys with close HVL and MFP values, the ratio of HVL values of the SPWAs with highest shielding properties (S6, S7, S9 and S10) to the SPWA with lowest one (S4) is shown in Fig. 4(b). It can be clearly seen that the ratio of HVL values of S9 to S4 are less than that of others, therefore S9 has highest shielding capability among the alloys. Like HVL, the ratio of lower MFP values (S6, S7 and S9) to the highest one (S4) is given in Fig. 4(c), too. Among the alloys, the lowest MFP ratio is seen for S9.

The interaction probability of per electron and per atom in a unit volume of any compound can be defined as ECS and ACS, respectively. ACS and ECS parameters with higher

values are desired for better shielding property. Changing of ACS and ECS values versus incident photon energies are given in Fig. 5(a-b). The reduction of photon-atom interaction probability at increasing photon energies can decrease the ACS and ECS values proportionally. It is obviously observed that ACS and ECS parameters of S4 alloy are lower than those of other alloys. In order to make the near values more visible, a specific energy region on the graph is given in a separate window and it is obtained that ACS and ECS results of the S9 alloy are higher than those of the other studied alloys.

The variations of Z_{eff} versus photon energy is given in Fig. 6(a). At low energies, maximum Z_{eff} values were obtained based on PE cross-section (Z^{4-5}). PE cross-section depend on $E^{-3.5}$ causes the reduction of values sharply at mid-energies. In high energy region, due to the PP cross-section varied with Z_2 the values increase gradually and be stable [4]. Compositions with different atomic numbers of elements are determinative on values of Z_{eff} . Z_{eff} values of the alloys which are composed of many elements with large differences in atomic numbers have greater fluctuations. This kind of fluctuations can be seen for the studied alloys. Maximum Z_{eff} values are obtained for S9 with content of W and Y (higher atomic number); while minimum Z_{eff} values are observed for S4 and S5 with content of Si and Ti (lower atomic number) among the SPWAs. Thus, it can be stated that the effective contribution on the increase of the Z_{eff} value is the amount of W in the alloys. S3, S6, S7, S8 and S10 alloys show close shielding properties in terms of Z_{eff} , but the highest value is obtained for S9.

Z_{eq} is the parameter changes depending on the only CS process [4]. The dependence of Z_{eq} values of the alloys are given in Fig. 6(b). Energy-dependent fluctuations can be also observed for Z_{eq} values of SPWAs comprised of elements with large differences in atomic numbers as with Z_{eff} . S9 alloy has the highest shielding property based on the Z_{eq} results.

The changes of EBF and EABF as a function of photon energies are shown in Figs. 7-8. At low energies, buildup factor values are small depending on the PE. EBF and EABF achieve their maximum at medium energies by the effect of a large number of photons scattered by the CS. At high energies, PP effect causes strong photon absorption and the buildup factors decrease [14, 16]. Thus, it is worthy to say that the buildup effect is observed dominantly at mid-energies. Higher MFP values are obtained at higher levels for EBF and EABF, due to the direct correlation between the photon scattering probability and the depth of penetration. An increase determined at ≈ 0.07 MeV for EBF and EABF of all studied alloys is because of the K-absorption edge of W [18]. Depending on the EBF and EABF values, the photons for S9 cluster relatively more than those for the others. It can be noted that the CS process is observed for S9 more.

Fast neutron attenuation potentials of the alloys were also calculated by Phy-X/PSD. It is obtained that FNRCS values of S2, S4, S5, S6 and S7 are 0.217, those of S1 and S3 are 0.216, those of S9 and S10 are 0.215, and that of S8 is 0.214. The lowest FNRCS is observed for S8.

4. Conclusion

In the study, the determination of the radiation attenuation parameters of SPWAs was performed with the Phy-X/PSD code in the range of 1 keV - 100 GeV. According to the outcomes, although, some of the parameters for the studied alloys have near values to each other, S9 has the highest shielding ability and S4 has the least one among the studied alloys. The alloys with higher amounts of W and Y have more shielding performances, while the alloys with lighter elements Ti and Si have less. It is also clear that HVL and MFP values of the studied alloys are lower than those of previously reported alloys. By the determination of ACS, ECS, Z_{eff} and Z_{eq} values, it is possible to say that S9 alloy shows the highest radiation attenuation, while S4 shows the lowest. In addition, whereas all the studied SPWAs have close FNRCS values, S2, S4, S5, S6 and S7 alloys have relatively higher values and all the alloys are suitable for neutron shielding. In conclusion, it can be mentioned that the SPWAs can be estimated as shielding materials for future fusion reactors among other features.

Conflict of interest statement:

The authors declare that they have no conflict of interest.

References

- [1] C. R. Hammond. *The Elements, in Handbook of Chemistry and Physics*. CRC Press, 2004.
- [2] A. Calvo, K. Schlueter, E. Tejado, G. Pintsuk, N. Ordás, I. Iturriza, R. Neu, J. Y. Pastor, and C. García-Rosales. "Self-passivating tungsten alloys of the system W-Cr-Y for high temperature applications". *International Journal of Refractory Metals and Hard Materials*, **73**:29, 2018.
- [3] D. Bachurina, X. Y. Tan, F. Klein, A. Suchkov, A. Litnovsky, J. Schmitz, J. Gonzalez-Julian, M. Bram, J. Willem Coenen, Y. C. Wu, and Ch. Linsmeier. "Self-passivating smart tungsten alloys for DEMO: a progress in joining and upscale for a first wall mockup". *Tungsten*, **3**:101, 2021.
- [4] A. Calvo, C. García-Rosales, F. Koch, N. Ordás, I. Iturriza, H. Greuner, G. Pintsuk, and C. Sarbu. "Manufacturing and testing of self-passivating tungsten alloys of different composition". *Nuclear Materials and Energy*, **9**:422, 2016.
- [5] C. García-Rosales, P. López-Ruiz, S. Alvarez-Martínez, A. Calvo, N. Ordás, F. Koch, and J. Brinkman. "Oxidation behaviour of bulk W-Cr-Ti alloys prepared by mechanical alloying and HIPing". *Fusion Engineer Design*, **89(7-8)**:1611, 2014.
- [6] T. Wegener, F. Klein, A. Litnovsky, M. Rasinski, F. Koch, and Ch. Linsmeier. "Development of yttrium-containing self-passivating tungsten alloys for future fusion power plants". *Nuclear Materials and Energy*, **9**:394, 2016.

- [7] X. Y. Tan, F. Klein, A. Litnovsky, T. Wegener, J. Schmitz, Ch. Linsmeier, J. W. Coenen, U. Breuer, M. Rasinski, P. Li, L. M. Luo, and Y. C. Wu. "Evaluation of the high temperature oxidation of W-Cr-Zr self-passivating alloys". *Corrosion Science*, **147**:201, 2019.
- [8] E. Sal, C. García-Rosales, K. Schlueter, K. Hunger, M. Gago, M. Wirtz, A. Calvo, I. Andueza, R. Neu, and G. Pintsuk. "Microstructure, oxidation behaviour and thermal shock resistance of self-passivating W-Cr-Y-Zr alloys". *Nuclear Materials and Energy*, **24**:100770, 2020.
- [9] A. Litnovsky, F. Klein, J. Schmitz, T. Wegener, Ch. Linsmeier, M. R. Gilbert, M. Rasinski, A. Kreter, X. Tan, Y. Mao, J. W. Coenen, M. Bram, and J. Gonzalez-Julian. "Smart first wall materials for intrinsic safety of a fusion power plant.". *Fusion Engineering and Design*, **136**:878, 2018.
- [10] M. I. Sayyed, F. Q. Mohammed, K. A. Mahmoud, E. Lacomme, K. M. Kaky, M. U. Khandaker, and M. R. Faruque. "Evaluation of Radiation Shielding Features of Co and Ni-Based Superalloys Using MCNP-5 Code: Potential Use in Nuclear Safety". *Applied Sciences*, **10**:7680, 2020.
- [11] Z. Aygun, M. Aygun, and N. Yarbaşı. "A study on radiation shielding potentials of green and red clayey soils in Turkey reinforced with marble dust and waste tire". *Journal of New Results in Science*, **10**:46, 2021.
- [12] Z. Aygun, N. Yarbasi, and M. Aygun. "Spectroscopic and radiation shielding features of Nemrut, Pasinler, Sarıkamis and İkizdere obsidians in Turkey: Experimental and theoretical study". *Ceramics International*, **47**:34207, 2021.
- [13] Z. Aygun and M. Aygun. "A theoretical study on radiation shielding characteristics of magnetic shielding alloys, Ni₈₀Fe₁₅Mo₅ and Ni₇₇Fe₁₄Cu₅Mo₄, by determining the photon attenuation parameters in the energy range of 15 keV - 100 GeV". *Karaelmas Science and Engineering Journal*, **11**:165, 2021.
- [14] Z. Aygun and M. Aygun. "Radiation shielding potentials of rene alloys by Phy-X/PSD code". *Acta Physica Polonica*, **141**:507, 2022.
- [15] Z. Aygun and M. Aygun. "Evaluation of radiation shielding potentials of Ni-based alloys, Inconel-617 and Incoloy-800HT, candidates for high temperature applications especially for nuclear reactors, by EpiXS and Phy-X/PSD codes". *Polytechnic Journal*, **26**:795, 2023.
- [16] Z. Aygun and M. Aygun. "A study on usability of Ahlat ignimbrites and pumice as radiation shielding materials, by using EpiXS code". *International Journal of Environmental Science and Technology*, **19**:5675, 2022.
- [17] Z. Aygun. "A study on radiation shielding characteristics of refractory high entropy alloys by EpiXS code". *Acta Physica Polonica*, **143**:66, 2023.
- [18] Z. Aygun and M. Aygun. "A study on radiation shielding abilities of some compounds of 3d transition elements by using Phy-X/PSD code". *Gazi University Journal of Science*, **36**:898, 2023.
- [19] G. Kilic, S. A. M. Issa, E. Ilik, O. Kilicoglu, and H. O. Tekin. "A journey for exploration of Eu₂O₃ reinforcement effect on zinc-borate glasses: Synthesis, optical, physical and nuclear radiation shielding properties". *Ceramics International*, **47**:2572, 2021.
- [20] S. A. M. Issa, A. M. Ali, H. O. Tekin, Y. B. Saddeek, A. Al-Hajry, H. Algarni, and G. Susoy. "Enhancement of nuclear radiation shielding and mechanical properties of YBiBO₃ glasses using La₂O₃". *Nuclear Engineering and Technology*, **52**:1297, 2020.
- [21] G. Almisned, D. S. Baykal, E. Ilik, M. Abuzaid, S. A. M. Issa, G. Kilic, H. M. H. Zakaly, A. Ene, and H. O. Tekin. "Tungsten (VI) oxide reinforced antimony glasses for radiation safety applications: A throughout investigation for determination of radiation shielding properties and transmission factors". *Heliyon*, **9**:e17838, 2023.
- [22] M. J. Berger and J. H. Hubbell. "XCOM: Photon Cross Sections Database". *National Institute of Standards and Technology Gaithersburg*, , 1987.
- [23] R. Nowotny. "XMuDat: Photon attenuation data on PC". *IAEA Report IAEA-NDS*, , 1998.
- [24] L. Gerward, N. Guilbert, K. B. Jensen, and H. Levring. "X-ray absorption in matter. Reengineering XCOM". *Radiation Physics and Chemistry*, **60**:23, 2001.
- [25] L. Gerward, N. Guilbert, K. B. Jensen, and H. Levring. "WinXCom—a program for calculating X-ray attenuation coefficients". *Radiation Physics and Chemistry*, **71**:653, 2004.
- [26] S. Agostinelli, J. Allison, K. Amako, J. Apostolakis, H. Araujo, P. Arce, M. Asai, D. Axen, S. Banerjee, G. Barrand, F. Behner, L. Bellagamba, and et al. "Geant4—a simulation toolkit". *Nuclear Instruments and Methods in Physics Research Section A: Accelerators, Spectrometers, Detectors and Associated Equipment*, **506**:250, 2003.
- [27] E. Sakar, Ö. F. Özpolat, B. Alım, M. I. Sayyed, and M. Kurudirek. "Phy-X/PSD: Development of a user friendly online software for calculation of parameters relevant to radiation shielding and dosimetry". *Radiation Physics and Chemistry*, **166**:1, 2020.
- [28] F. C. Hila, A. A. Astronomo, C. A. M. Dingle, J. F. M. Jecong, A. M. V. Javier-Hila, M. B. Z. Gili, Ch. V. Balderas, G. E. P. Lopez, N. R. D. Guillermo, and A. V. Amorsolo Jr. "EpiXS: A Windows-based program for photon attenuation, dosimetry and shielding

- based on EPICS2017 (ENDF/B-VIII) and EPDL97 (ENDF/B-VI.8)". *IEEE Transactions on Plasma Science*, **182**:109331, 2021.
- [29] K. S. Mann and S. S. Mann. "Py-MLBUF: Development of an online-platform for gamma-ray shielding calculations and investigations". *Annals of Nuclear Energy*, **150**:107845, 2021.
- [30] P. López-Ruiz, N. Ordás, I. Iturriza, M. Walter, E. Gaganidze, S. Lindig, F. Koch, and C. García-Rosales. "Powder metallurgical processing of self-passivating tungsten alloys for fusion first wall application". *Journal of Nuclear Materials*, **442**:S219, 2013.
- [31] A. Litnovsky, T. Wegener, F. Klein, Ch. Linsmeier, M. Rasinski, A. Kreter, B. Unterberg, M. Vogel, S. Kraus, U. Breuer, C. Garcia-Rosales, A. Calvo, and N. Ordas. "Smart alloys for a future fusion power plant: First studies under stationary plasma load and in accidental conditions". *Nuclear Materials and Energy*, **12**:1363, 2017.
- [32] M. I. Sayyed, A. Ibrahim, M. A. Abdod, and M. S. Sadeq. "The combination of high optical transparency and radiation shielding effectiveness of zinc sodium borate glasses by tungsten oxide additions". *Journal of Alloys and Compounds*, **904**:164037, 2022.
- [33] M. Dong, S. Zhou, X. Xue, M. I. Sayyed, D. Tishkevich, A. Trukhanov, and C. Wang. "Study of comprehensive shielding behaviors of chambersite deposit for neutron and gamma ray". *Progress in Nuclear Energy*, **146**:104155, 2022.
- [34] C. Xiang, E. H. Han, Z. M. Zhang, H. M. Fu, J. Q. Wang, H. F. Zhang, and G. D. Hu. "Design of single-phase high-entropy alloys composed of low thermal neutron absorption cross-section elements for nuclear power plant application". *Intermetallics*, **104**:143, 2019.
- [35] Y. Harima, Y. Sakamoto, S. Tanaka, and M. Kawai. "Validity of the geometric-progression formula in approximating gamma-ray buildup factors". *Nuclear Science and Engineering*, **94**:24, 1986.
- [36] Y. Harima. "An historical review and current status of buildup factor calculations and applications". *Radiation Physics and Chemistry*, **41(4-5)**:631, 1993.
- [37] ANSI/ANS 6.4.3 Gamma ray Attenuation Coefficients and La Grange Park Illinois Buildup Factors for Engineering Materials, American Nuclear Society. " ". , 1991.
- [38] E. Sakar. "Determination of photon-shielding features and build-up factors of nickel-silver alloys". *Radiation Physics and Chemistry*, **172**:1, 2020.
- [39] J. Wood. *Computational methods in reactor shielding*. Elsevier, 2013.
- [40] I. I. Bashter. "Calculation of Radiation Attenuation Coefficients for Shielding Concretes". *Annals of Nuclear Energy*, **24**:1389, 1997.